

EVALUATION OF EDDY VISCOSITY TURBULENCE MODELS TO PREDICT CONVECTIVE HEAT TRANSFER

Christian HESCHL^{1*}, Kiao INTHAVONG² and Jiyuan TU²

¹ Fachhochschulstudiengänge Burgenland, University of Applied Science, Steinamangerstraße 21, Pinkafeld 7423, Austria

² School of Aerospace, Mechanical and Manufacturing Engineering, RMIT University, PO Box 71, Plenty Road, Bundoora, Victoria 3083, Australia

*Corresponding author, E-mail address: Christian.Heschl@fh-burgenland.at

ABSTRACT

Within the CFD-optimization process of thermal energy conversion systems an accurate prediction of the convective heat transfer is required. Because of the lower computational effort and the numerical stability, eddy viscosity turbulence models are often used. Besides the different velocity and time scales the eddy viscosity concept offers a lot of modifications such as variable turbulent Prandtl number, stagnation point, entrainment and near wall correction.

Based on the $k-\epsilon$, $k-\omega$, and v^2-f turbulence models the potential of the customised modifications will be discussed. The studies include different free convection and room airflow situations. Moreover the flow around a heated obstacle will be presented.

According to the validation results it is shown that the most accurate computations can be obtained with the v^2-f model if the stagnation point and the entrainment correction are used, while the $k-\epsilon$ and $k-\omega$ based turbulence models underestimate the convective heat transfer.

NOMENCLATURE

C_1, C_2	model constants in the v^2f model
$C_{\epsilon 1}, C_{\epsilon 2}$	model constants in the ϵ -equation
C_{η}, C_L	model constants in the length scale equation
C_{lim}	model constant in the realizability constrain
C_μ	turbulent viscosity model constant
f	relaxation parameter in the v^2f model
g_i	gravitational acceleration
k	turbulent kinetic energy
L	turbulent length scale
m_{CFD}	RANS based computed mass flow rate
m_{DNS}	DNS computed mass flow rate from
S_{ij}	strain rate tensor
P_k	production rate due to turbulent stresses
P_b	production rate due to buoyancy
Re_y	turbulent Reynolds number
T	turbulent time scale
u_t	turbulent velocity scale
v^2	normal stress in the fictive wall-normal direction
β	volumetric thermal expansion coefficient
ϵ	dissipation rate
λ_ϵ	blend factor
μ	dynamic viscosity
μ_t	dynamic turbulent viscosity
σ	turbulent Prandtl number
ρ	density
θ	non-dimensional temperature

INTRODUCTION

The fluid flow dynamics in industrial processes are dominated by turbulent momentum and heat exchange processes. Hence an accurate prediction of the convective heat transfer rate requires a reliable and numerical efficiency computation of the turbulent transport mechanism. Due to the numerical robustness and the low computational effort, linear eddy viscosity models are often used for industrial applications. These models are based on the Boussinesq analogy between the viscous and turbulent stresses. Similar to the molecular viscosity, the turbulent structures are characterized by a turbulent length and a velocity scale. Alternatively a turbulent length scale and a turbulent time scale can be used.

In analogy to the molecular approach the product of the time scale and the quadratic velocity scale can be described by the turbulent viscosity as:

$$\mu_t \sim \rho \cdot u_t^2 \cdot T \quad (1)$$

In contrast to the molecular viscosity the turbulent viscosity isn't a fluid property. It depends on the flow structure and must be determined accordingly. In the literature different approaches are used to quantify the characteristic values (e.g. Wilcox, 2006, Launder and Spalding, 1972). Standard models use the turbulent kinetic energy k as an equivalent quantity for the turbulent velocity scale u_t . Because of the well-known overestimation of the turbulent shear stresses near the wall, this fundamental approach is not broadly accepted. Within the turbulent boundary layer, the velocity scale should be proportional to the spanwise turbulent normal stress. This behaviour is illustrated for a two-dimensional channel flow in Figure 1. The turbulent viscosity is determined by the Boussinesq hypotheses ($\nu_t = -u'v' dy/du$).

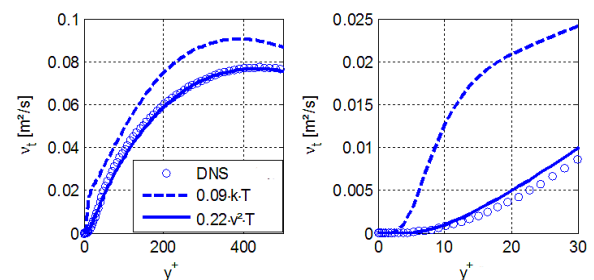


Figure 1: Comparison of different turbulent velocity scales for the prediction of the turbulent viscosity in a 2D channel ($Re_\tau=944$, DNS from Del Alamo et al., 2004).

If the turbulent kinetic energy k is used ($0.09kT$) the turbulent viscosity is dramatically over-estimated near the wall. However if the turbulent normal stress in the spanwise direction is utilized ($0.22v^2T$) a better agreement with the DNS data can be observed. This more realistic approach suggests that such models are more universal and able to provide more accurate results over a wide range of applications. However in its practical use it can be shown that such models can lead to an under-prediction of the entrainment and spreading rate in turbulent free jets. Hence in this paper, a modified v^2 -f turbulence model which avoids the under-prediction of the turbulent momentum exchange in free shear flows will be presented and its performance over extensive convective heat transfer cases is discussed.

MODEL DESCRIPTION

Durbin (1991) proposed a v^2 -f model which consists of four transport equations to determine the turbulent viscosity. These are the turbulent kinetic energy, the dissipation rate and two addition equations - one for the imaginary turbulent normal stress and one for the elliptical relaxation. The latter considers the elliptical nature of the correlation between the fluctuations of the pressure and the velocity gradients. This enables the considerations of wall reflection effects without locally dependent algebraic relations. Pressure reflections which can reach far into the flow domain and therefore have a strong non-locality can be taken into account.

In this paper, a modified version (from Lien and Kalitzin, 2001) of the original v^2 -f model is used. In contrast to the model from Durbin (1991) the modified version allows a segregated solution of all transport equations. For this reason it is particularly well suited for implementation in standardized CFD-solvers. In addition the proposed improvements from Davidson et al. (2003) to ensure that the imaginary velocity scale is smaller than $2/3k$ is utilized. The transport equations are given as follows:

$$\frac{\partial \rho k}{\partial t} + \frac{\partial \rho k u_i}{\partial x_i} = \frac{\partial}{\partial x_j} \left[\left(\mu + \frac{\mu_t}{\sigma_k} \right) \frac{\partial k}{\partial x_j} \right] + P_k + P_G - \rho \varepsilon \quad (2)$$

$$\frac{\partial \rho \varepsilon}{\partial t} + \frac{\partial \rho \varepsilon u_i}{\partial x_i} = \frac{\partial}{\partial x_j} \left[\left(\mu + \frac{\mu_t}{\sigma_\varepsilon} \right) \frac{\partial \varepsilon}{\partial x_j} \right] + \frac{C_{\varepsilon 1} (P_k + P_G) - C_{\varepsilon 2} \rho \varepsilon}{T} \quad (3)$$

$$\frac{\partial \rho v^2}{\partial t} + \frac{\partial \rho v^2 u_i}{\partial x_i} = \rho \Theta_{kf} - 6 \frac{v^2}{k} \rho \varepsilon + \frac{\partial}{\partial x_j} \left[\left(\mu + \frac{\mu_t}{\sigma_k} \right) \frac{\partial v^2}{\partial x_j} \right] \quad (4)$$

$$\Theta_{kf} = \text{MIN} \left(k f, C_2 \frac{P_k + P_G}{\rho} - \frac{1}{T} \left((C_1 - 6)v^2 - \frac{2}{3}k(C_1 - 1) \right) \right) \quad (5)$$

$$L^2 \frac{\partial^2 f}{\partial x_j^2} - f = \frac{C_1}{T} \left(\frac{v^2}{k} - \frac{2}{3} \right) - C_2 \frac{(P_k + P_G)}{k \rho} - \frac{1}{T} \left(6 \frac{v^2}{k} - \frac{2}{3} \right) \quad (6)$$

$$\mu_t = C_\mu \rho v^2 T \quad \text{and} \quad P_G = -\beta g_i \frac{\mu_t}{\sigma_i} \frac{\partial T}{\partial x_i} \quad (7)$$

To avoid singularities in the conservation equations near the wall limitations for the turbulent time scale T and the turbulent length Scale L are introduced by the Kolmogorov variable according equation (8) and (9).

$$T = \max \left(\frac{k}{\varepsilon}, 6 \sqrt{\frac{\mu / \rho}{\varepsilon}} \right) \quad (8)$$

$$L = C_L \max \left(\frac{k^{3/2}}{\varepsilon}, C_\eta \frac{\mu^{3/4}}{\rho^{3/4} \varepsilon^{1/4}} \right) \quad (9)$$

To avoid the stagnation point anomaly additional restrictions for the turbulent time and length scales are proposed in the literature. A particular discussion about the influences to the computational results and to the numerical stabilities is presented in Sveningsson (2003). He pointed out that the additional limitation of the turbulent length scale can produce numerical instabilities if the relaxation equation is solved. Furthermore he showed that the computational results in the stagnation point area are mainly influenced by the time scale limiter. For this reason in this paper only the determination of the time scale that includes an additional limiter to avoid the stagnation point anomaly is used (see equation (10)).

$$T = \min \left[\max \left(\frac{k}{\varepsilon}, 6 \sqrt{\frac{\mu / \rho}{\varepsilon}} \right), \frac{C_{\text{lim}} k}{\sqrt{6} C_\mu v^2 S} \right] \quad (10)$$

For the length scale the conventional limiter according equation (9) is used. The boundary conditions at the walls are

$$u_i = 0, k = 0, v^2 = 0, f = 0, \varepsilon = 2 \frac{\mu}{\rho} \left(\frac{k_p}{y_p^2} \right) \quad (11)$$

and for the inlet the values must be specified directly for each transport equation. For the elliptical operator f , a homogeneous Neumann boundary condition is used.

The proposed model constants from Lien and Kalitzin (2001) are the same as the standard k - ε model except for the determination of the model constant $C_{\varepsilon 1}$ which adjusts the value for the near wall and the core flow as:

$$C_{\varepsilon 1} = 1.4 \left(1 + 0.050 \sqrt{\frac{k}{v^2}} \right) \quad (12)$$

Although in many cases this equation is used, this leads to unrealistic results for the turbulent shear stresses. For example in a plane wall jet the v^2 -f model will compute a v^2/k ratio of about 0.35 which leads to a $C_{\varepsilon 1}$ value of 1.52 from equation (12). However for the turbulent plane jet a $C_{\varepsilon 1}$ value of 1.4 is required. Consequently this produces under-predictions of the entrainment and spreading rates ($dy_{1/2}/dx \approx 0.08$ instead 0.10-0.11). For this reason a blend function which allows an individual adjustment of the model constant $C_{\varepsilon 1}$ for the near wall and outer boundary layer is proposed:

$$C_{\varepsilon 1} = \lambda_\varepsilon C_{\varepsilon 1 \text{ wall}} + (1 - \lambda_\varepsilon) C_{\varepsilon 1 \text{ free shear flow}} \quad (13)$$

$$\lambda_\varepsilon = \frac{1}{2} \left[1 + \tanh \left(\frac{\text{Re}_y - \text{Re}_y^*}{A} \right) \right] \quad (14)$$

$$\text{Re}_y = \frac{\rho \sqrt{k} y_{\text{wall}}}{\mu} \quad \text{Re}_y^* = 500 \quad A = \frac{|0.2 \text{Re}_y^*|}{\tanh(0.98)} \quad (15)$$

The equations (13), (14) and (15) represent a simple function which interpolate the $C_{\varepsilon 1}$ value between the $C_{\varepsilon 1 \text{ wall}}=1.59$ for the near wall and $C_{\varepsilon 1 \text{ free shear flow}}=1.40$ for the free shear flow region. Hence more accurate results for free shear flows can be obtained. In this paper the model constants are summarized in Table 1.

C_μ	$C_{\varepsilon 2}$	C_1	C_2	σ_k	σ_ε	σ_l	C_L	C_η	C_{lim}
0.22	1.9	1.4	0.3	1.0	1.3	0.85	0.23	70	0.6

Table 1: Used model constants.

The implementation of the v^2 -f model into the commercial CFD code Fluent was performed using its User Defined Function (UDF) interface. The implementation complies with the rule that the linear portion of the source terms always supplies negative contributions, to get a stable turbulence model (more details can be found in Patankar, 1980).

The computational mesh for all models was suitable for a low-Re calculation where the dimensionless distance to the wall of the first grid cell is $y^+ < 1$. Therefore for the k - ε model, the low-Re extension proposed by Wolfstein (1969) and for the $k\omega$ -SST the low-Re corrections were used. For all test cases a grid independence test based on the Richardson extrapolation (Fletcher, 2000) was carried out. In all cases a discretization error of less than 1% could be detected for turbulence and velocity quantities.

To determine the validity of the proposed modified v^2 -f model, five different flow scenarios are used for analysis. These include traditional benchmarks such as flow separation, convective heat transfer, natural convection flow and flow around obstacles. To allow direct comparison with other turbulence models, the calculation results (V2F-MOD) in addition to the data measured by the standard k - ε model including Enhanced Wall Treatment (SKE) and the $k\omega$ turbulence model with shear-stress transport equation (KW-SST) from Menter (1993) compared. All calculations were performed with a low-Re grid ($y^+ < 1$) and with the commercial CFD code Fluent (Fluent, 2007).

RESULTS AND DISCUSSION

Two dimensional channel flow

Due to the availability of extensive DNS data and its simple geometry the flow through a two-dimensional channel is particularly suitable for validation of near wall behaviour. The computational geometry is shown in Figure 2. To reduce the computational effort periodic conditions are applied at the inlet and outlet, while at the centre of the channel a symmetric boundary condition is used.

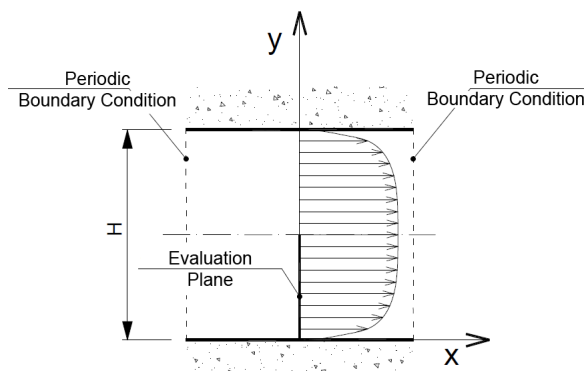


Figure 2: Computational domain of the 2D channel flow.

To summarize the validation results for a wide range of turbulent Reynolds number (Re_τ) in Figure 3 the computed

mass flow through the 2D channel is compared with the DNS data from Moser et al. (1999) in terms of normalized values (the value 1 conforms with the DNS data). The V2F model with the $C_{\varepsilon 1}$ constants proposed from Lien and Kalitzin (2001) over predicts the mass flow rates and thus underestimates the wall shear stresses. The deviations of the mass flow rates are not constant and depend on the turbulent Reynolds number. With the introduced approach a significantly better results can be achieved. The V2F-MOD matches the DNS over the whole turbulent Reynolds numbers well.

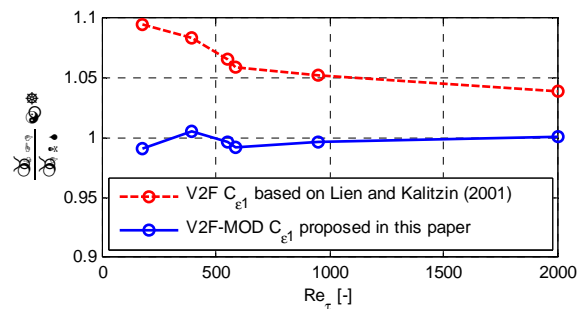


Figure 3: Comparison of the computed mass flow rates.

Two dimensional room airflow

To validate a simple non-isothermal air flow, the experimental data of Blay et al. (1992) is used for the velocity and the temperature distribution. The geometry (Figure 4) is a square cavity having dimensions of $L=1040\text{mm}$, $h=18\text{mm}$, $t=24\text{mm}$. Air at 15°C enters the inlet at a velocity of 0.57m/s . The top and side walls are set at 15°C while the bottom wall is set at 35.5°C .

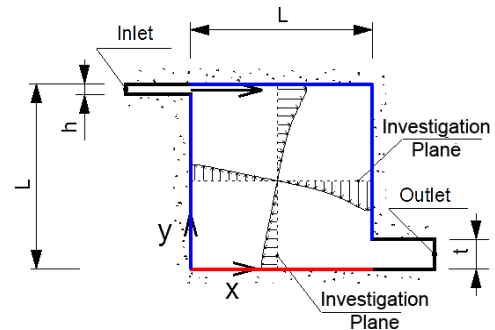


Figure 4: Geometry of square cavity with plane jet

Distribution profiles of the velocity (u_y/u_0) and temperature (θ) are shown in Figure 5. The velocity profile is normalized by the inlet velocity while the non-dimensional temperature, θ is defined as $(T-T_h)/(T_v-T_h)$ where T_h and T_v are the temperatures of the hot horizontal and cold vertical wall, respectively. The results show that the KW-SST model underestimates the entrainment and high flow velocities in the immediate vicinity of the wall. The SKE and the V2F-MOD show much better agreement with the velocity profiles. However with respect to the temperature distribution the V2F-MOD model provides the best results.

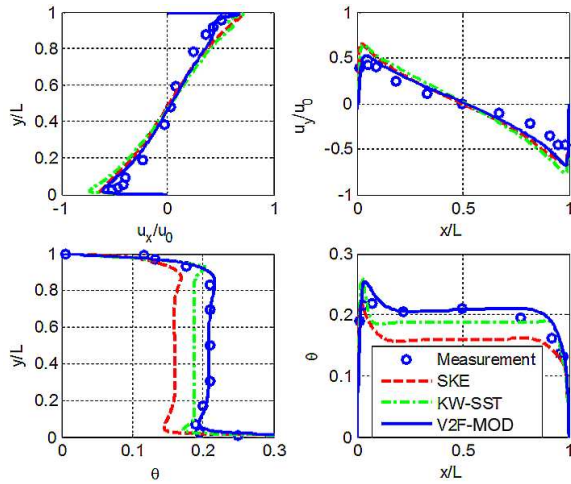


Figure 5: Velocity and temperature profiles for plane wall jet in a square cavity.

Vertical free convection

In this example, the natural convection on a hotter vertical surface ($T_w=25^\circ\text{C}$) was investigated under an isothermal environment having a temperature of $T=20^\circ\text{C}$. The geometric model for this test case was created by Kriegel (2005) where the dimension of the vertical wall is 6-meters, and the floor (treated as adiabatic) is 1.5-m (Figure 6). The profile of the heat transfer rate along the vertical wall height was calculated for this buoyant flow. Near the floor the heat transfer asymptotes towards 25W/m^2 and decreases away from the floor. The V2F-MOD model provides significantly better performance over the SKE and KW-SST models as it is able to reproduce a local minima at $y\sim 1.5\text{m}$ with an increase in q with increase in y . The KW-SST and SKE do not show any minima but a smooth parabolic profile.

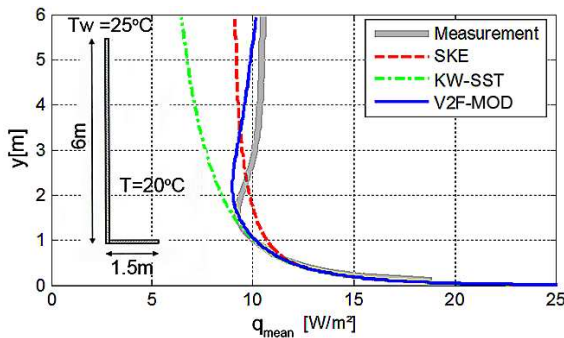
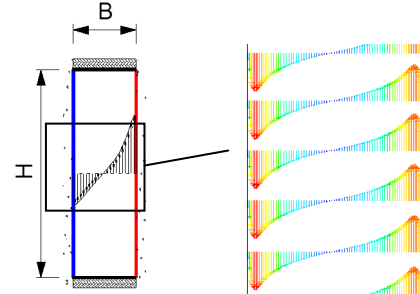


Figure 6: Schematic and heat transfer rate profile results for vertical free convection. Measurement data according to Raithby and Hollands (1998).

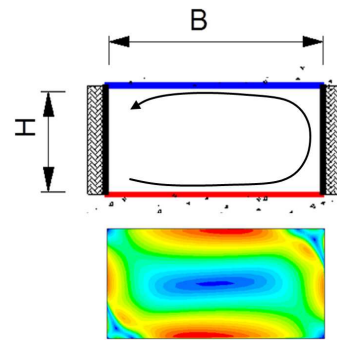
Free convection in an enclosed cavity

Buoyancy-induced convective flows in a vertical and horizontal enclosed cavity are used to evaluate free convection (Figure 7). The dimensions of the vertical cavity is $H=2.18\text{m}$ and $B=0.0762\text{m}$, with adiabatic top and bottom walls, and the left wall with $T_L=0^\circ\text{C}$ and right wall temperature varying, $T_R=1-100^\circ\text{C}$. The dimensions of the horizontal cavity is $H=3\text{m}$ and $B=6\text{m}$, with adiabatic left and right walls, and the top wall with $T_L=0^\circ\text{C}$ and right wall ranging in temperature $T_R=1-100^\circ\text{C}$.

The calculated Nusselt number Nu (measure of heat transfer) as a function of Rayleigh number, Ra is plotted for the different varying temperatures ($1-100^\circ\text{C}$ at the hotter surface). Both the SKE and KW-SST models under-predict the heat transfer rates and at higher Ra , the discrepancy gets worse. The V2F-MOD provides significant improvements and the predicted results fall in the range of the experimental data for both the vertical and horizontal enclosure.



(a) vertical enclosure geometry and velocity contour



(b) horizontal enclosure geometry and velocity contour

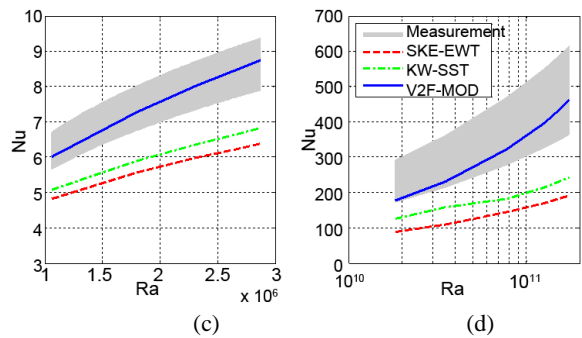


Figure 7: Schematic and velocity contour for (a) vertical enclosure (b) horizontal enclosure. Nusselt number profile results for (c) vertical enclosure, measurement data according to Elsherbiny et al. (1982) (d) horizontal enclosure, measurement data according to Probert et al. (1970).

Flow around an heated obstacle

The flow of cooler air passing over a heated obstacle is experimentally visualised using LIF (laser-induced fluorescence) which is used to evaluate the turbulence models. Figure 8 shows the geometry of the flow where a downwards flow of cooler air passes over a heated obstacle. The inlet profile is a developed flow within the enclosed region having a width of $B=0.38\text{m}$.

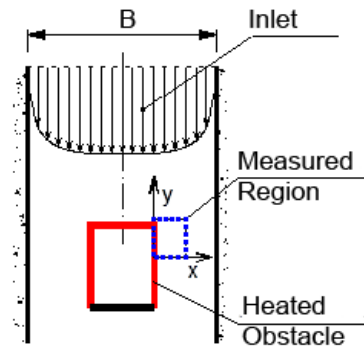


Figure 8: Schematic of flow over a heated obstacle. Blue dotted region is used to visualise the temperature distribution.

The measured and simulated temperature distributions in the vicinity of the upper right hand corner of the obstacle are shown in Figure 9. The forced flow around the heater produces a forced mixing effect where the natural buoyant convection that rises from the heated obstacle is impeded by the downwards momentum flux from the inlet. The measured temperature contour shows a curved “tail” of warmer air that points downwards. The high dissipative nature of the SKE model and its significantly high production of turbulent kinetic energy due to the large stagnation point region, shows high temperatures remaining near the wall and no heated air ‘tail’ can be found in the region away from the wall. The KW-SST model has a similar contour plot but with a shorter temperature ‘tail’. The V2F-MOD is able to capture to tail effect and provides the best results of the three models.

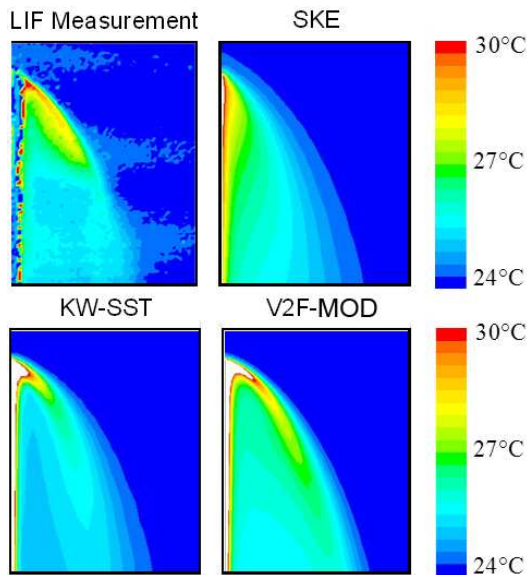


Figure 9: Temperature contour plot in the vicinity of the right hand upper corner of the heated object (see dotted blue box in Figure 8).

Barrel of Ilmenau

The world’s largest experiment (7.0 m x 6.3 m) to study highly turbulent thermal convection of air with high spatial and temporal resolution is the experimental test rig named the ‘Barrel of Ilmenau’ which represents a large-scale Rayleigh-Bènard convective flow. A hot plate is

installed between the floor and a suspended cooling plate, and the air is set into turbulent motion. Due to the freely suspended cold plate which is mounted on a crane, the aspect ratio can be altered. A schematic of the Barrel of Ilmenau is Figure 10.

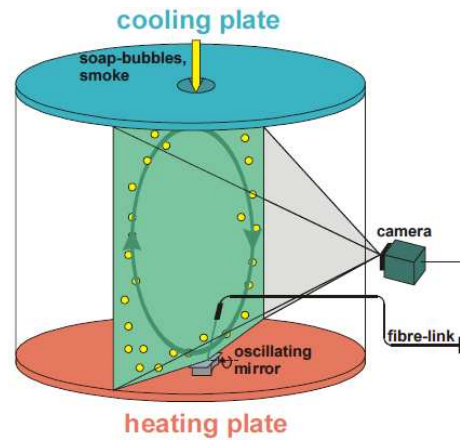


Figure 10: Schematic of the ‘Barrel of Ilmenau’ and the measurement setup.

The experimental data that is produced through the Technical University of Ilmenau can attain very high Rayleigh numbers and performs detailed non-contact measurements and visualizations of flow inside this cylindrical domain for verification of indoor airflow computations.

To reconstruct this three-dimensional model, a large number of cells would have been necessary. Therefore, a half-cylinder with the same dimensions and a plane of symmetry was used. Following the guidelines in the literature (Du Puits, 2007) with the aspect ratio $\Gamma = 1.13$, the diameter of 7.15 m and height 6.3 m was modeled. A sketch of the model is given in Figure 11. The completed mesh of the half cylinder comprises 1.4598 million cells.

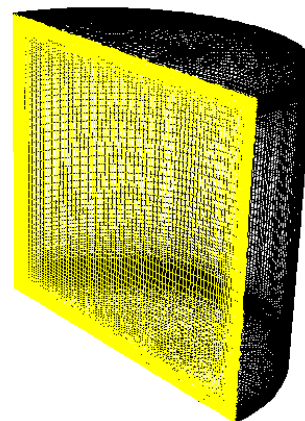


Figure 11: CFD model of the ‘Barrel of Ilmenau’

The results in Figure 12 show that both the SKE and KW-SST models underpredict the heat transfer rate and this is more significant as the Ra number gets larger. The V2F-MOD has much closer agreement with the experimental data. Its Nu number values are slightly greater than the experimental data.

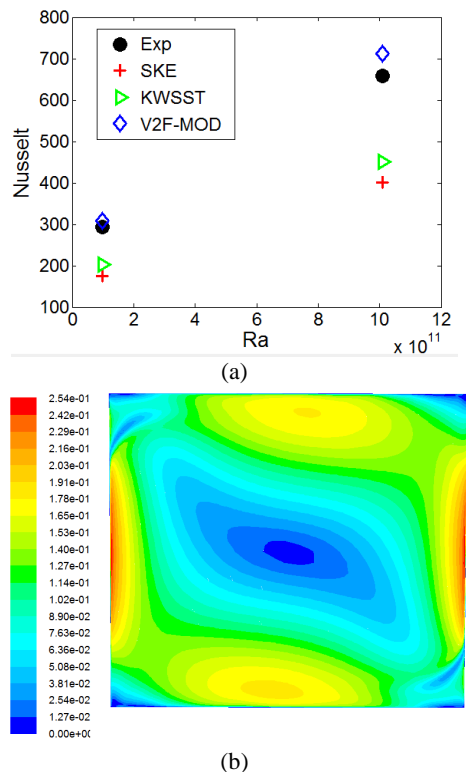


Figure 12: (a) Corresponding Nusselt (Nu) at different Rayleigh (Ra) number for the different turbulence model performance (b) velocity contour [m/s] taken at the symmetry plane showing the natural convection currents.

CONCLUSION

In this work a standard $k-\epsilon$, $k-\omega$ -SST and a modified v^2-f turbulence model for a number of standard test cases is presented to determine the temperature distribution, and heat transfer rate due to buoyant flow found in natural convection, and forced convection. It was shown that the turbulent exchange of momentum in free shear flows is significantly underestimated when using the classical model constants for the ϵ -equation. The reason for this is the equation for determining the proportionality of the production term in the ϵ -equation, which has been calibrated for near-wall shear flows and thus modifications are needed for free shear flows. For this reason a modification is proposed which allows an individual adjustment of the dissipation rate production away from the wall.

Validation of the modified v^2-f model was based on different flow situations. It was shown that the modified v^2-f model can successfully capture the isothermal and non-isothermal air flow phenomena in convective heat transfer processes and flow around obstacles.

REFERENCES

BLAY, D., MERGUI, S., NICULAE, C. (1992), "Confined turbulent mixed convection in presence of a horizontal buoyant wall jet" *Fundamentals of Mixed Convection*, AS HTD-Vol. 213, 65-72

DAVIDSON, L., NIELSEN, P. V. and SVENINGSSON, A., (2003), "Modification of the V2F model for computing the flow in a 3d wall jet" *Turbulence Heat and Mass Transfer* 4, 577-584.

DEL ALAMO, J. C., JIMENEZ, J., ZANDONADE, P., MOSER, R. D. (2004), "Scaling of the energy spectra of turbulent channels" *J. Fluid Mech.* 500, 135-144.

DU PUITTS, R., RESAGK, Ch., TILGNER, A., BUSSE, F. H., THESS, A., (2007), "Structure of thermal boundary layers in turbulent Raleigh-Bernard convection" *J. Fluid Mech.*, Vol. 572, page 231-254.

DURBIN, P., (1991), "Near-wall turbulence closure modeling without damping functions" *Theoretical and Computational Fluid Dynamics* 3, 1-13.

ELSHERBINY, S.M., (1982), "Heat Transfer by Natural Convection Across Vertical and Inclined Air Layers", *Journal of Heat Transfer*, Vol. 104, page 96-102.

FLETCHER, C. A. J., (2000), "Computational Techniques for Fluid Dynamics I. Fundamental and General Techniques" *Springer Berlin Heidelberg NewYork*, ISBN 3-54053058-4

FLUENT (2007), "Fluent 12 User's Guide" *Fluent Inc. Centerra Resource Park, Lebanon*.

KRIEGEL, M., (2005), „Experimentelle Untersuchung und numerische Simulation eines Quellluftsystems“ *Dissertation, TU Berlin, Tenea Verlag, Berlin*, page 73.

LAUNDER, B.E. and SPALDING, D.B., (1972), "Lectures in Mathematical Models of Turbulence" *Academic Press, London, England*.

LIEN, F. and KALITZIN, G., (2001), "Computations of transonic flow with the v2f turbulence model" *International Journal of Heat and Fluid Flow*, Vol. 22, 53-61.

MENTER, F.R., (1993), "Zonal Two Equation $k-\omega$ Turbulence Models for Aero-dynamical Flows" *AIAA paper No. 93-2906, 24th Fluid Dynamics Conference, Florida*, 1-21.

PATANKAR, S.V., (1980), "Numerical Heat Transfer and Fluid Flow" *Hemisphere Publishing Corporation, NewYork Washington Philadelphia London*, ISBN 0-89116-522-3.

PROBERT, S.D., BROOKS, R.G., DIXAN, M., (1970), *Chem. Process Eng. Heat Transfer Survey*, page 35-42.

RAITHBY, G., HOLLANDS, K., (1998), "Natural Convection" *Handbook of Heat Transfer*, 3rd Edition. McGraw-Hill, New York.

SVENINGSSON, A., (2003), "Analysis of the Performance of different v2-f Turbulence Models in a Stator Vane Passage Flow" *Dissertation. Department of Thermo and Fluid Dynamics, Chalmers University of Technology, Sweden*.

WILCOX, D.C., (2006), "Turbulence Modeling for CFD", *Third Edition, DCW Industries, Inc.*, ISBN 978-1-928729-08-2, USA San Diego.

WOLFSHTEIN, M., (1969), "The Velocity and Temperature Distribution in One-Dimensional Flow with Turbulence Augmentation and Pressure Gradient" *International Journal of Heat and Mass Transfer* 12:301-318.